



HAL
open science

Ranking genome-wide correlation measurements improves microarray and RNA-seq based global and targeted co-expression networks

Franziska Liesecke, Dimitri Daudu, Rodolphe Dugé de Bernonville, Sébastien Besseau, Marc Clastre, Vincent Courdavault, Johan-Owen de Craene, Joël Crèche, Nathalie Giglioli-Guivarc'h, Gaëlle Glevarec, et al.

► To cite this version:

Franziska Liesecke, Dimitri Daudu, Rodolphe Dugé de Bernonville, Sébastien Besseau, Marc Clastre, et al.. Ranking genome-wide correlation measurements improves microarray and RNA-seq based global and targeted co-expression networks. *Scientific Reports*, 2018, 8 (1), pp.10885 - 10885. 10.1038/s41598-018-29077-3 . hal-01865148

HAL Id: hal-01865148

<https://hal.science/hal-01865148>

Submitted on 31 Aug 2018

HAL is a multi-disciplinary open access archive for the deposit and dissemination of scientific research documents, whether they are published or not. The documents may come from teaching and research institutions in France or abroad, or from public or private research centers.

L'archive ouverte pluridisciplinaire **HAL**, est destinée au dépôt et à la diffusion de documents scientifiques de niveau recherche, publiés ou non, émanant des établissements d'enseignement et de recherche français ou étrangers, des laboratoires publics ou privés.

SCIENTIFIC REPORTS



OPEN

Ranking genome-wide correlation measurements improves microarray and RNA-seq based global and targeted co-expression networks

Franziska Liesecke, Dimitri Daudu, Rodolphe Dugé de Bernonville, Sébastien Besseau, Marc Clastre, Vincent Courdavault , Johan-Owen de Craene , Joel Crèche, Nathalie Giglioli-Guivarc'h, Gaëlle Glévarec, Olivier Pichon & Thomas Dugé de Bernonville 

Co-expression networks are essential tools to infer biological associations between gene products and predict gene annotation. Global networks can be analyzed at the transcriptome-wide scale or after querying them with a set of guide genes to capture the transcriptional landscape of a given pathway in a process named Pathway Level Coexpression (PLC). A critical step in network construction remains the definition of gene co-expression. In the present work, we compared how Pearson Correlation Coefficient (PCC), Spearman Correlation Coefficient (SCC), their respective ranked values (Highest Reciprocal Rank (HRR)), Mutual Information (MI) and Partial Correlations (PC) performed on global networks and PLCs. This evaluation was conducted on the model plant *Arabidopsis thaliana* using microarray and differently pre-processed RNA-seq datasets. We particularly evaluated how dataset \times distance measurement combinations performed in 5 PLCs corresponding to 4 well described plant metabolic pathways (phenylpropanoid, carbohydrate, fatty acid and terpene metabolisms) and the cytokinin signaling pathway. Our present work highlights how PCC ranked with HRR is better suited for global network construction and PLC with microarray and RNA-seq data than other distance methods, especially to cluster genes in partitions similar to biological subpathways.

Constructing global gene co-expression networks is a popular approach to highlight transcriptional relationships (edges) between genes (vertices). The ‘Guilt-by-Association’ (GBA) principle supposes that genes sharing similar functions are preferentially connected and aims at predicting new functions for proteins by determining how their respective encoding genes are co-expressed with others using a reference dataset containing known gene functions such as the Gene Ontology (GO)¹. Defining edges connecting genes remains a critical step in global co-expression network construction. Expression data (microarray or RNA-seq) are used to construct expression matrices (genes \times samples) and to calculate a distance or a similarity for each possible gene pair. The resulting pairwise distance matrix is then thresholded to obtain an adjacency matrix that discriminates relevant edges. Only edges with a distance below (or a similarity above) the set threshold are considered significant and retained for network construction. The procedure is expected to remove non biologically relevant gene associations while retaining the relevant ones and can be assessed with any reference dataset. Alternatively, guide gene sets may be used to extract more human-readable information from large networks in a process named Pathway-Level Coexpression (PLC)^{2–7}. This approach aims at capturing the best transcriptional associations of a gene set and at highlighting functional gene groups such as known subpathways in this set. There are two types of approaches to determine transcriptional associations of genes: those that are supervised and those that are unsupervised. Supervised approaches such as regression and machine learning based methods require a prior knowledge which is used as a training dataset to recover biologically relevant gene associations and are used to infer regulatory networks, *i.e.* to uncover preferential and sequential interactions of a gene over the others. The superiority of

Université de Tours, EA2106 Biomolécules et Biotechnologies végétales, Tours, 37200, France. Correspondence and requests for materials should be addressed to T.D.d.B. (email: thomas.duge@univ-tours.fr)

supervised methods in extracting potential physical regulatory interactions between genes has been demonstrated using simulated and real *E. coli* and *S. cerevisiae* subnetworks⁸. This study has revealed that prediction accuracy is higher with smaller networks and concluded that inferring genome-scale networks remains elusive unless performing a feature selection step to reduce inference problem size (because of the under determined nature of current expression datasets). Contrastingly, unsupervised approaches are used to capture transcriptional associations in co-expression networks. Although these associations may not be causative, a higher propensity of strongly correlated genes is a valuable information which may have a biological meaning in a cellular or physiological context. Among the unsupervised methods, four are commonly used and have been thoroughly tested. The first approach is Mutual Information (MI) which measures a statistical dependence between two variables⁸. It is based on density function estimates and has been shown to perform well with non linear relationships⁹. The second approach which relies on integrating multiple transcriptional associations is Partial Correlation (PC). First-order PCs may be simply calculated using the following equation $R_{xy.z} = \frac{R_{yx} - (R_{yz})(R_{xz})}{\sqrt{(1 - (R_{yz}^2))(1 - (R_{xz}^2))}}$ with R_{xy}

R_{yz} and R_{xz} the simple correlation coefficients between genes x and y, y and z, x and z respectively¹⁰, but such computations may be very time consuming for large datasets. In this case, PCs should rather be calculated by multiple linear regression including a feature selection step¹¹. In this way, PCs aim at explaining a gene's expression profile by a small number of strongly correlated genes after eliminating those less correlated that do not significantly explain this gene's expression profile. The two last methods are Correlation Coefficients (CCs), either Pearson CC (PCC) or Spearman CC (SCC), which are the classical estimators of linear transcriptional relationship among genes^{11,12}. CCs are 2-dimensional distance measurements because a CC between two genes does not take into account the expression of the remaining transcripts in the whole transcriptome. To improve CCs, it has been proposed to recursively correct expression values according to a neural network algorithm with a weighted CC matrix until an equilibrium is reached between input and output expression¹³. Used on a small dataset, this method was useful to uncover interaction networks even for genes included in background cellular activities. Neural networks have however been reported to be computationally expensive for larger datasets¹⁴. Another improvement was to use ranked CCs instead of raw values. Ranking CC implies that for every gene, all CCs are calculated with the N-1 remaining genes (where N is the number of genes) and are ranked from 1 to N. Within a pair of genes A and B, rank(A to B) differs from rank(B to A) because the two genes display different expression profiles and different relationships with the remaining transcripts in the transcriptome. Two related ranking methods have been developed. One is mutual ranking (MR, geometric mean of the two ranks) which has been shown to improve GO term recovery with PCC using large microarray data from Arabidopsis, Human, mouse and rat¹⁵. MR has been successfully used in multispecies analysis of co-expression modules¹⁶. Another is Highest Reciprocal Ranking (HRR, maximum value of the two ranks)¹⁷. MR and HRR are thought to be more integrative than unranked CCs because they depend on other CC values around that of a gene pair. It might also be expected that ranking CCs partially correct for the "range restriction effect" observed for CCs leading to robust correlations for high variance genes only¹⁸. Although not as robust as supervised methods, unsupervised methods can efficiently capture relevant gene associations as previously shown⁹. These authors have shown that non parametric CC and MI calculations were more efficient than PCC on a small dataset. Among other unsupervised methods, SCC calculations have been similarly shown to outperform other distance measurements in Human expression data¹⁹. In this case, SCC were calculated from RNA-seq or microarray data in order to construct several smaller networks subsequently aggregated to yield the final network. We firmly believe that genome-scale networks inferred with CCs, especially when combined with a ranking procedure, are helpful to find new associations between genes. Although CCs are not efficient in detecting non linear associations⁹, gene-to-gene relationships have been predicted to be essentially linear²⁰ suggesting that CCs are valuable distance measurements. To date, there is no clear evaluation of how ranked CCs affect genome-scale network reconstruction with RNA-seq data in comparison with other unsupervised methods. We evaluated ranked CC, raw CC, MI, and PC performance in global and targeted network construction using Arabidopsis microarray and differentially processed RNA-seq expression data (Fig. 1). By using unsupervised methods, our aim was to highlight transcriptional associations between genes from an expression dataset. Querying genome-scale datasets is a useful preliminary step in identifying genes involved in biological pathways. Because correlation does not imply causality, the study of regulatory interactions or sequential orders through supervised methods is beyond the scope of our work. Although specific dedicated conditions are useful to find groups of intercorrelated genes²¹, large scale expression matrices were used here in order to increase the number of different experimental conditions and obtain robust averaged correlations. This approach should be useful for non-model species which global transcriptional landscapes have to be studied. Performance was measured as network ability to capture biologically relevant gene associations found in a Gene Ontology (GO) annotation reference set but also to correctly cluster guide genes in PLC. Global network quality was first evaluated according to the different dataset \times distance measurement combinations. The resulting global networks were next interrogated in PLC analyses with five different guide gene sets corresponding to four different metabolic pathways and one signaling pathway. Whereas metabolic pathways have relatively clearly defined and partially linear partitions, signaling pathways usually involve post transcriptional regulations and a more intricate organization, which might render gene transcriptional associations less evident. We looked at the dataset \times distance measurement combinations optimizing pathway reconstruction and maximizing co-occurrence quality between microarray and RNA-seq networks. Our results show that, of the six methods evaluated, PCC ranked with HRR generated the best biologically relevant networks according to initial guide gene representation and clustering in distinct modules. In addition, it offers the possibility to merge subgraphs obtained by microarrays and RNA-seq to generate high confidence networks.

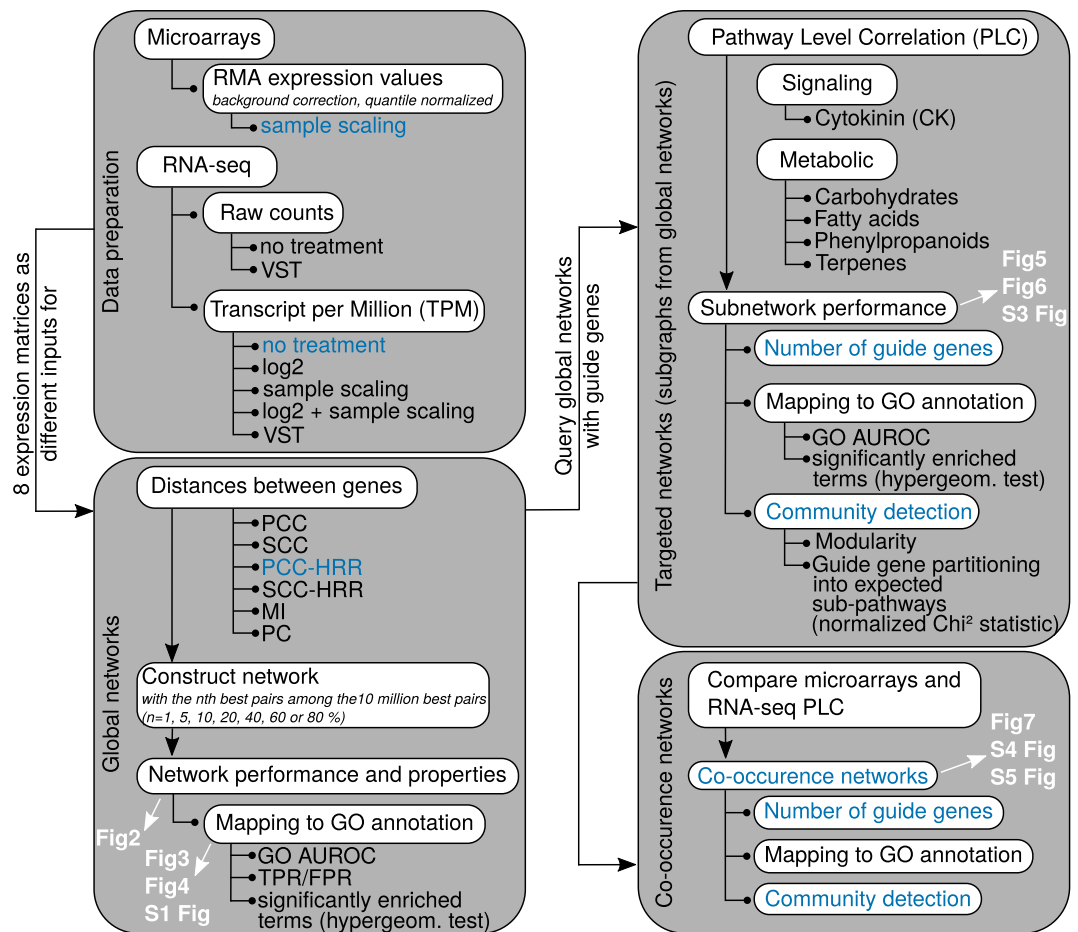


Figure 1. Workflow for global and targeted network analyses. One microarray dataset and a RNA-seq dataset prepared according to 7 normalization procedures were used to generate eight expression matrices analyzed with six different distance measurements (Pearson's or Spearman's Correlation Coefficient, unranked or ranked with HRR, Mutual Information (MI) or Partial Correlations (PC)) to obtain 48 distance matrices. Each of these matrices was thresholded to obtain global networks at different confidence thresholds. Global networks were evaluated and also queried with specific guide gene sets reflecting 5 different pathways in a process named Pathway Level Correlation (PLC). The resulting subnetworks were evaluated and used to construct co-occurrence networks between microarray and RNA-seq datasets. In white are indicated the figures corresponding to the different steps analyzed. Dataset \times distance combinations are indicated in blue and characteristics that are improved by these combinations.

Results

Inferring global co-expression networks and comparing correlation measurements. Large co-expression networks were obtained by varying the confidence threshold (correlation value above or rank below) within lists containing the 10 million best gene pairs from eight different datasets and six data measurement combinations (Fig. 1). Each of the 10 million best pair lists was filtered at different confidence thresholds (1, 5, 10, 20, 40, 60 or 80% best pairs from these lists) to evaluate the effect of network size on performance. Expression datasets included a microarray-based expression matrix and seven RNA-seq based expression matrices normalized with different methods to evaluate their effect on network inference: transcript per Million (TPM), log₂ TPM, sample scaled (ss) TPM, ss log₂ TPM, raw counts, variance stabilized transformed (VST) raw counts and VST-TPM. The six distance measurements were: raw PCC, raw SCC, PCC-HRR, SCC-HRR, PC and MI. Each network performance was considered as a network ability to capture edges corresponding to functional associations found in the GO reference dataset and was evaluated in 4 different ways (Fig. 2): GO term enrichment (GO terms that are significantly enriched with gene pairs from the co-expression network), a ROC curve constructed with TPR and FPR calculated for each confidence threshold and two ROC analyses based on the GBA concept, an average 3-fold cross validated neighbor voting (NV) AUROC and a global AUROC. AUROCs correspond to Area Under Receiver Operating Characteristic curves calculated for every network either from each GO (with three test sets obtained after hiding part of the gene labels, NV AUROC corresponding to the average of AUROCs for all GO terms) or the whole annotation dataset (global AUROC). AUROCs are used as global indicators of a dataset performance, a value of 0.5 indicating a random attribution of labels in the network and a value of 1 indicating a perfect match with the reference dataset. AUROC > 0.6 may be considered as moderate¹⁹. In global

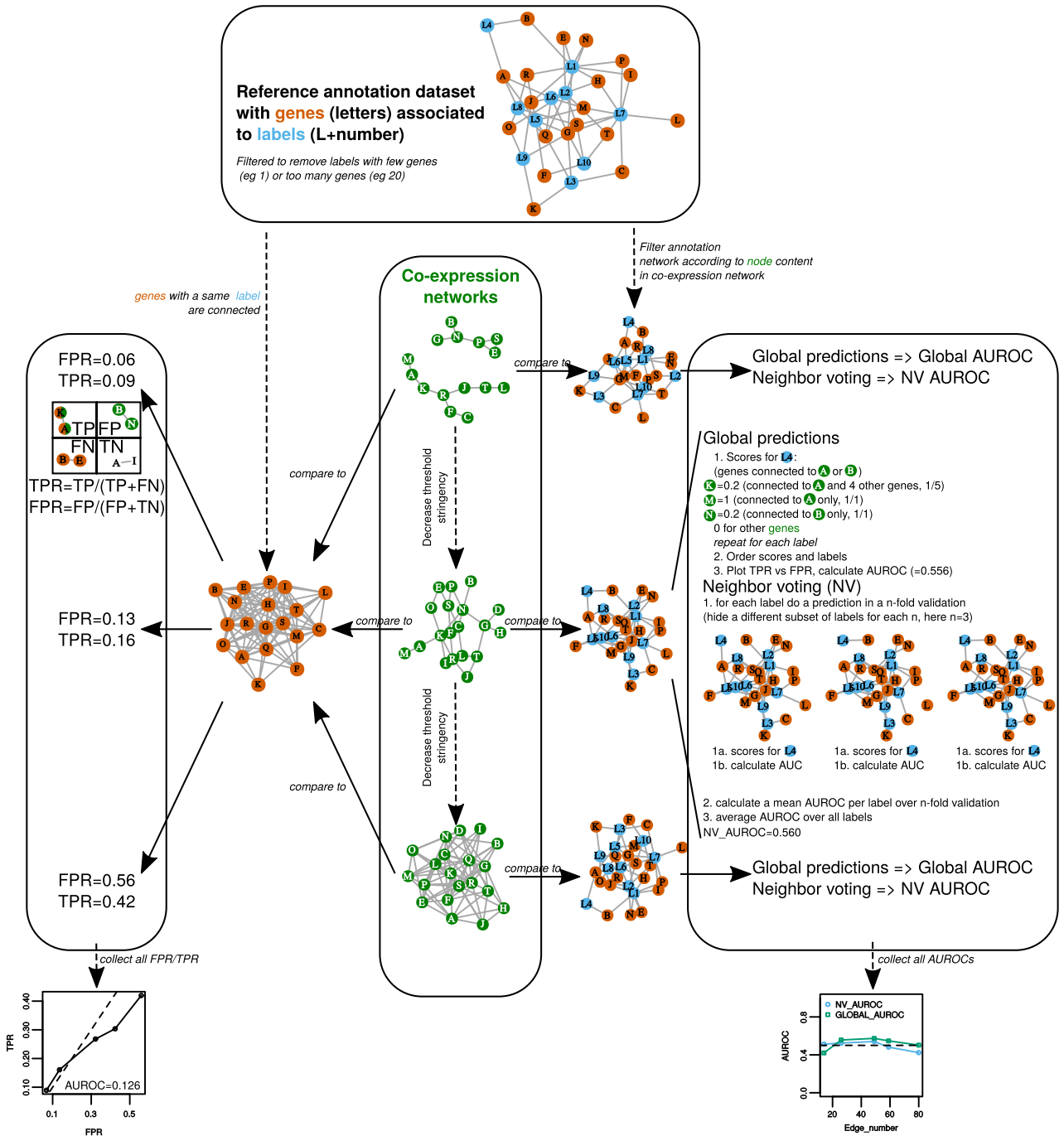


Figure 2. Network performance. This small example describe strategies to evaluate networks according to a reference functional annotation. Co-expression networks were obtained for each dataset × distance measurement combination (Fig. 1) at different confidence thresholds, resulting in networks increasing in size with lower stringency. A total evaluation was made with True Positive Rate (TPR) vs False Positive Rate (FPR) analysis (left panel) by classifying edges as True positives (TP), False Positives (FP), False Negatives (FN) or True Negatives (TN). Single network evaluation was performed by calculating AUROCs with the EGAD R package, either as a global prediction or using a neighbor voting (NV) algorithm with a 3-fold cross validation (right panel). All indicated values are in accordance with the small networks in this example. In addition to these 3 evaluations (FPR vs TPR, global AUROC and NV AUROC), GO term significant enrichment was statistically tested with a hypergeometric distribution (not shown in this example).

TPR vs FPR curves, the line extending from (0,0) to (1,1) has an AUROC = 0.5 and points above this line indicate more predictive networks than a random selection (Fig. 2). The GO annotation table was filtered to perform these analyses by removing weakly represented or non-specific GO terms (>5 or <100 genes).

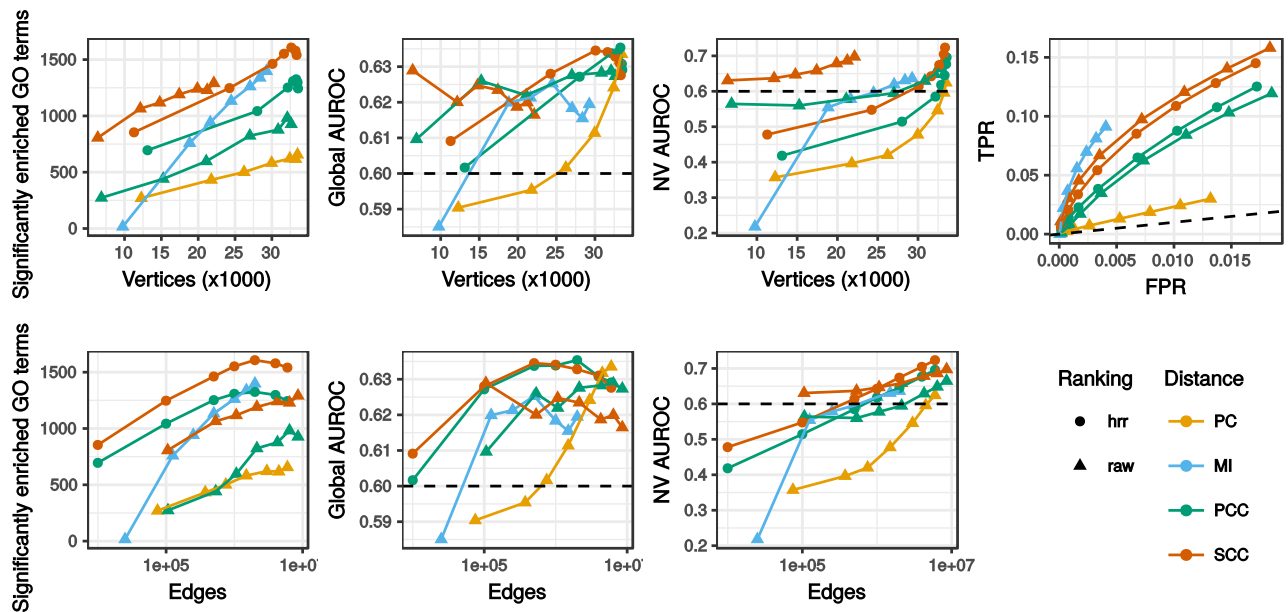


Figure 3. Global network characteristics. Only results for the RNA-seq TPM dataset without further normalization are shown. The horizontal dashed line indicates a 0.6 AUROC value taken as a threshold separating good and poor network predictability. In the $TPR = f(FPR)$ panel, the dashed line corresponds to a random selection (with $AUROC < 0.5$). This panel is partial and the highest FPRs correspond to 10 million gene pairs.

Figure 3 displays TPM network evaluation at different confidence thresholds and Fig. 4 shows networks having 1 million of edges across all dataset \times distance combinations. Metrics for all other dataset \times distance measurement combinations are presented in Supplementary Fig. 1. All networks combined, pairwise correlations between enriched GO counts, global and NV AUROC performance metrics were moderate (Spearman's $\rho > 0.4$) but significant ($p < 0.001$) indicating these three performance metrics evaluated networks in different ways. The highest correlation was observed between NV AUROC and enriched GO counts ($\rho = 0.70$, $p < 0.001$) showing their consistency. The NV AUROC was the most positively correlated with edge number ($\rho = 0.55$, $p < 0.001$) suggesting that decreasing the confidence threshold and adding more edges in networks did not result in a significant increase in false positives. This was confirmed by the partial ROC curves (obtained for a maximum FPR at 10 million edges) drawn from the TPR and FPR (Fig. 3, Supplementary Fig. 1), where up to 10 million best pairs, TPR increased faster than FPR. Although counts of significantly enriched GO terms were positively correlated to NV AUROC, we observed a slight decline in the largest networks which might reveal a saturation in these enriched GO terms. It is possible that with the hypergeometric testing, some GO classes are fully enriched in smaller networks leading to a decrease in their significance as network size increases. The global AUROC displayed a very low variation (min = 0.55, average = 0.61, max = 0.68) and was significantly correlated to vertex number ($\rho = 0.43$, $p < 0.001$) only. This observation suggests that the global AUROC is not an appropriate measure in our case.

At equivalent edge numbers, different distance measurements generated networks varying considerably in vertex number (Fig. 4A, Supplementary Fig. 1). Considering all datasets and distance measurements, raw PCC, raw SCC and MI resulted on average in fewer vertices and higher node degree (vertex number/node degree: 13,164/511, 9,986/465 and 14,074/468 respectively) than PCC-HRR, SCC-HRR or PC (26,645/116, 24,731/124 and 23,966/166 respectively). This trend was clearly observed when setting an edge number to 1 million (Fig. 4A). Expression networks constructed from microarrays, TPM, TPM log₂, and counts displayed very similar ROC curves: PC based networks followed random predictions (NV AUROC = 0.5) and the other distance measurements were above the random prediction with similar AUC (Supplementary Fig. 1). This was confirmed for PC by NV AUROC and enriched GO term counts. Performance of the other distance measurements in the global TPR/FPR curves did not exactly match that measured with AUROCs. Taking the TPM dataset as an illustration (Fig. 3), the MI ROC curve was above the others while NV AUROC for similar edge numbers was slightly below that measured for SCC. This was probably due to differences in network topologies (see above) and the procedures underpinning the two evaluations. The global TPR/FPR curve does not measure a network predictability *per se* as NV AUROC does and considering any gene pair sharing a same GO term as valid could have overestimated TP (Fig. 2). As a general trend, raw PCC and raw SCC generated smaller networks than PCC-HRR and SCC-HRR but displayed similar TPR/FPR curves, *i.e.* for a similar performance, HRR-ranked CC networks had more vertices and fewer edges than raw CC based networks (Fig. 3). CC ranked with HRR always generated relevant networks for TPM ss, TPM log₂ ss, TPM VST and counts VST, which was not the case for raw CC (Supplementary Fig. 1). These normalizations induced strong biases in CC distribution as revealed by thresholds used to obtain the 10 million best pairs (Supplementary Table 1) but these biases were compensated by HRR. For these four normalization methods, thresholds used to get the best co-expressed gene lists were > 0.9 . Contrastingly, thresholds

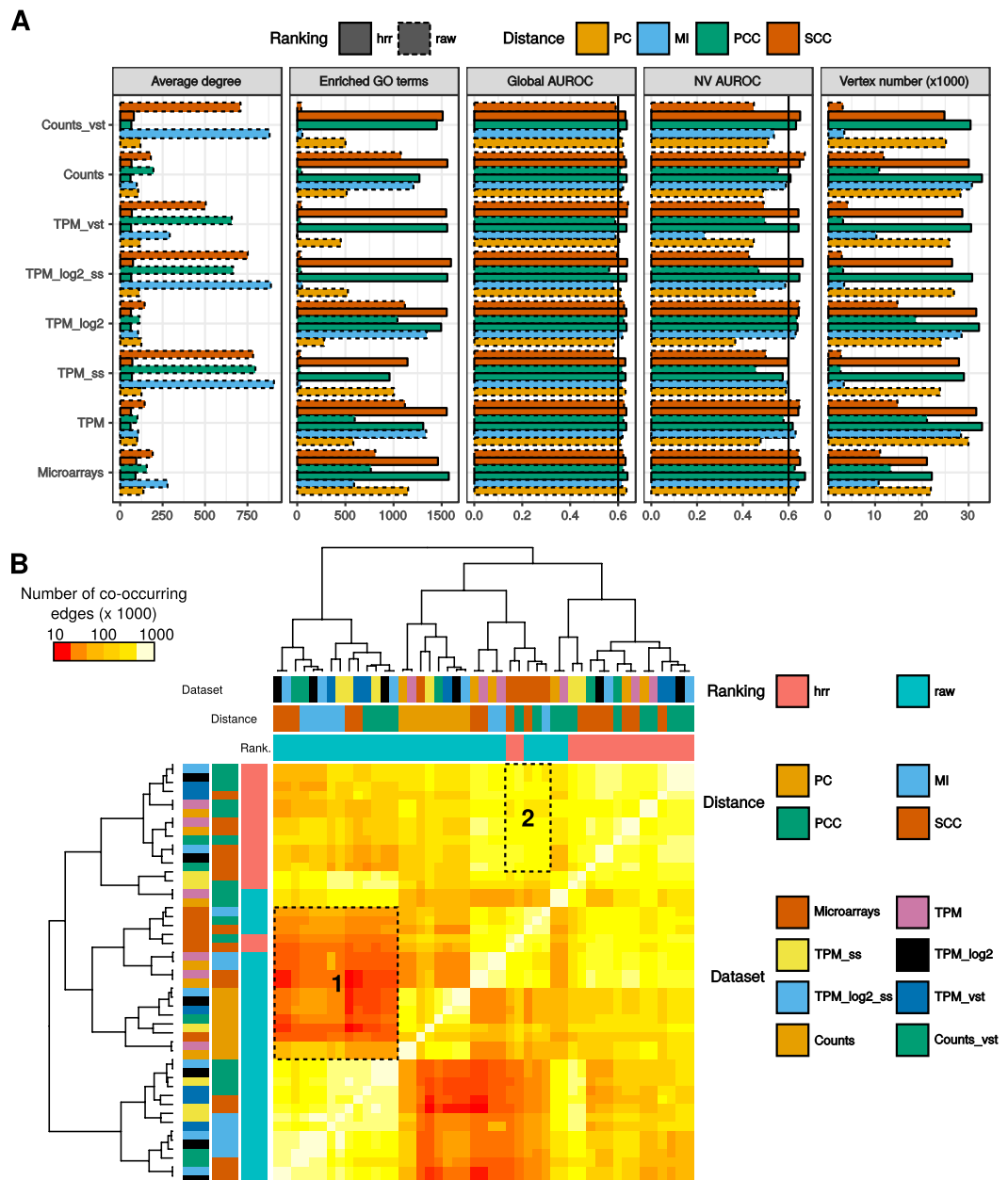


Figure 4. Comparison of dataset \times distance measurement combinations for networks with a million gene pairs. Network topology and performance in GO recovery were analyzed (**A**). Vertical lines at 0.6 indicate AUROCs above which network predictability can be considered as moderate. Co-occurring edges were also counted in every possible comparison between 2 networks (**B**). Area 1 corresponds to RNA-seq networks having few genes in common with PC networks and microarrays networks and area 2 to combinations maximizing edge co-occurrence between microarray and RNA-seq.

were <0.7 for the other methods (without VST or scaling) and it indicated a bias in CC distribution towards 1. However using ranked CCs with VST or scaling normalizations resulted in HRR thresholds in range with that obtained for the other normalization methods (around 1300, at the exception of TPM ss at 2200). In addition to this bias in CC values, VST or sample scaling normalization procedures were associated with higher node degree (average node degree of 712 vs 114 for other normalization procedures; Welch Two Sample t-test $p < 5 \times 10^{-7}$) and lower performance (both in the number of significantly enriched GO terms, average 36 vs 1,145, $p < 9 \times 10^{-12}$, and NV AUROC, average of 0.47 vs 0.62, $p < 0.001$) (Fig. 4A and Supplementary Fig. 1). These results clearly shows that network topologies were strongly impacted by VST and sample scaling procedures which resulted in less vertices that were more tightly connected together with a loss of GO term capture. Taken together, these results revealed that HRR CCs are able to generate complete genome-wide networks with good performances similar to other classical measures such a MI and PC. Node degree AUROC measures whether genes are more likely associated according to their number of connections rather than to their function. A positive correlation was found

between NV AUROC and degree AUROC ($\rho = 0.47, p < 2e-16$) indicating that highly predictive networks (NV AUROC > 0.7) also had a higher node degree AUROC. Node degree AUROC was generally under 0.55. We therefore considered that in our conditions, this bias was only limited. Concerning edge co-occurrence between the different dataset \times distance combinations, the lowest conservation was observed with raw (MI, PCC and SCC) RNA-seq datasets and PC networks and microarrays networks (Fig. 4B, area 1). Interestingly, many edges were conserved between VST or sample scaled normalized datasets when correlations were calculated with raw PCC (4B; below block 1). This was probably due to their particular topologies (see above) having few vertices very tightly connected. More co-occurring edges were found when microarray networks were compared to RNA-seq networks obtained with CC-HRR (mean of 97,646 vs 25,277; Fig. 4B, area2). This indicated that microarrays and RNA-seq networks were more comparable when obtained with HRR, reinforcing their validity. The previous section focused on global network properties. Community detection procedures can be applied to such global networks to cluster tightly connected genes into modules. In our case, we rather used a knowledge-driven approach known as Pathway-Level Coexpression (PLC) to extract gene pairs associated within a given pathway (Supplementary Fig. 2). PLC are particularly interesting in plants for example to decipher incomplete specialized metabolic pathways. It aims at capturing a transcriptional landscape for genes known to be involved in a given pathway, in order to highlight their organization as well as finding new genes (transporters, transcription factors, ...) associated with the process. In the next part, we evaluated the ability of all previous networks to capture relevant information associated with four metabolic and one signaling pathways. We selected two primary metabolic pathways (carbohydrate and fatty acid metabolisms), two specialized (secondary) pathways (phenylpropanoid and terpenoid metabolisms) and the cytokinin signaling pathway.

Assessing PLC quality: trade-off between GO term representation and guide genes. The PLC procedure is expected to cluster together guide genes with many co-expressed genes ('associated genes') and to reflect the subpathway organization (Fig. 5A). For PLC, we systematically removed all genes showing a degree value of 1 (*i.e.*, those connected to only one guide gene). However we included edges between associated genes if they were found among edges retained at the selected threshold. Using five pathways (Table 1, Fig. 5B, Supplementary Table 2 and Supplementary Fig. 3), we extracted five PLC from the global networks generated above to determine the best suitable dataset \times distance measurement combinations. All pathways have modular structures with gene sets forming specific sub-pathways (also called partitions or modules). We expected that PLC would be able to reconstruct such a partitioning, by connecting guide genes with associated genes. Pathways investigated here are typically reaction chains involving several enzymes working in coordination and having no direct effect on the transcription of their gene mates. As a consequence, specific sub-pathways are expected to form coordinated and specific correlation units highlighted within specific experimental conditions²¹. Concerning the signaling pathway, some of the query gene products could directly bind the promoter of other guide genes to control their expression²². Its study may clearly require a regulatory network approach but we investigated how co-expression network performed with such a signaling pathway. The phenylpropanoid pathway contains a core module composed of 3 genes leading to a precursor used by 3 other distinct subpathways²³⁻²⁶ (Fig. 5B, Table 1, Supplementary Table 2). The three other metabolic pathways, carbohydrates, fatty acids and terpenoids, were structured in modules as described on the KEGG database²⁷ (Table 1, Supplementary Table 2). The fatty acid pathway contains 97 genes divided into 6 modules. The central carbohydrate metabolism contains 202 genes partitioned in 8 modules. Finally, the terpene pathway has 64 genes partitioned into 6 modules. Pathway organizations were used as indicated in the KEGG database (apart from phenylpropanoid pathway which was manually curated from our previous work) and compared to PLC subnetworks. The plant cytokinin (CK) pathway is known to regulate many processes in plant physiology and is hierarchically organized in three levels: a histidine kinase receptor, a transducer (histidine phosphotransfer proteins) and a response regulator (type A/B/C) which may act as a transcription factor²⁸ (Table 1, Supplementary Table 2). Although CK pathway members are relatively well known, each level is represented by several members which may have specific roles and it is still unclear how they biologically interact with each other to drive a specific physiological response. We expected that PLC would group some of these actors according to specific physiological responses. CK pathway includes both transcription activating and repressing activities (via response regulators) and post-transcriptional (phosphorylations) and would therefore be an excellent test of PLC applicability on associations expected to be more complex than in metabolic pathways. In addition, we included other histidine kinases integrating other signals and known to crosstalk with the CK pathway²⁹. We therefore included 2 ethylene receptors, ETR1 and ERS1 to determine whether they could be clustered with CK histidine kinase. The initial pathway was not partitioned into sub-pathways but rather into 5 levels (receptor, transducer, type A/B/C response regulator) because interactions between specific actors of each level are not completely understood.

Subgraphs of global networks were constructed for each pathway by retrieving edges involving at least one guide gene and were partitioned into communities with a fast greedy algorithm designed to maximize network modularity and which has been shown to extract relevant communities from large networks³⁰. We compared guide gene distribution in these communities to target subpathways using a normalized χ^2 test which values range from 0 to 1, 1 being the expected partition and 0 a random partition of guide genes or very few guide genes (Fig. 5A). All networks having a χ^2 p -value > 0.05 were considered to have a χ^2 statistic equal to 0. PLC performance in recovering GO terms was evaluated by counting significantly enriched GO terms and by calculating a NV AUROC for each network. A good PLC was expected to contain a large number of guide genes and to have both a good score in grouping them into expected partitions (high normalized χ^2 value) and a good score in overall biologically relevant edge recovery (NV AUROC > 0.6). We first analyzed correlations between all these metrics (NV AUROC, number of guide genes and χ^2 statistic) together with two topological metrics (mean node degree and modularity), for each pathway separately (Fig. 5B). Strongest correlations were observed between NV AUROC and mean node degree ($\rho > 0.5, p < 0.001$) and between modularity and

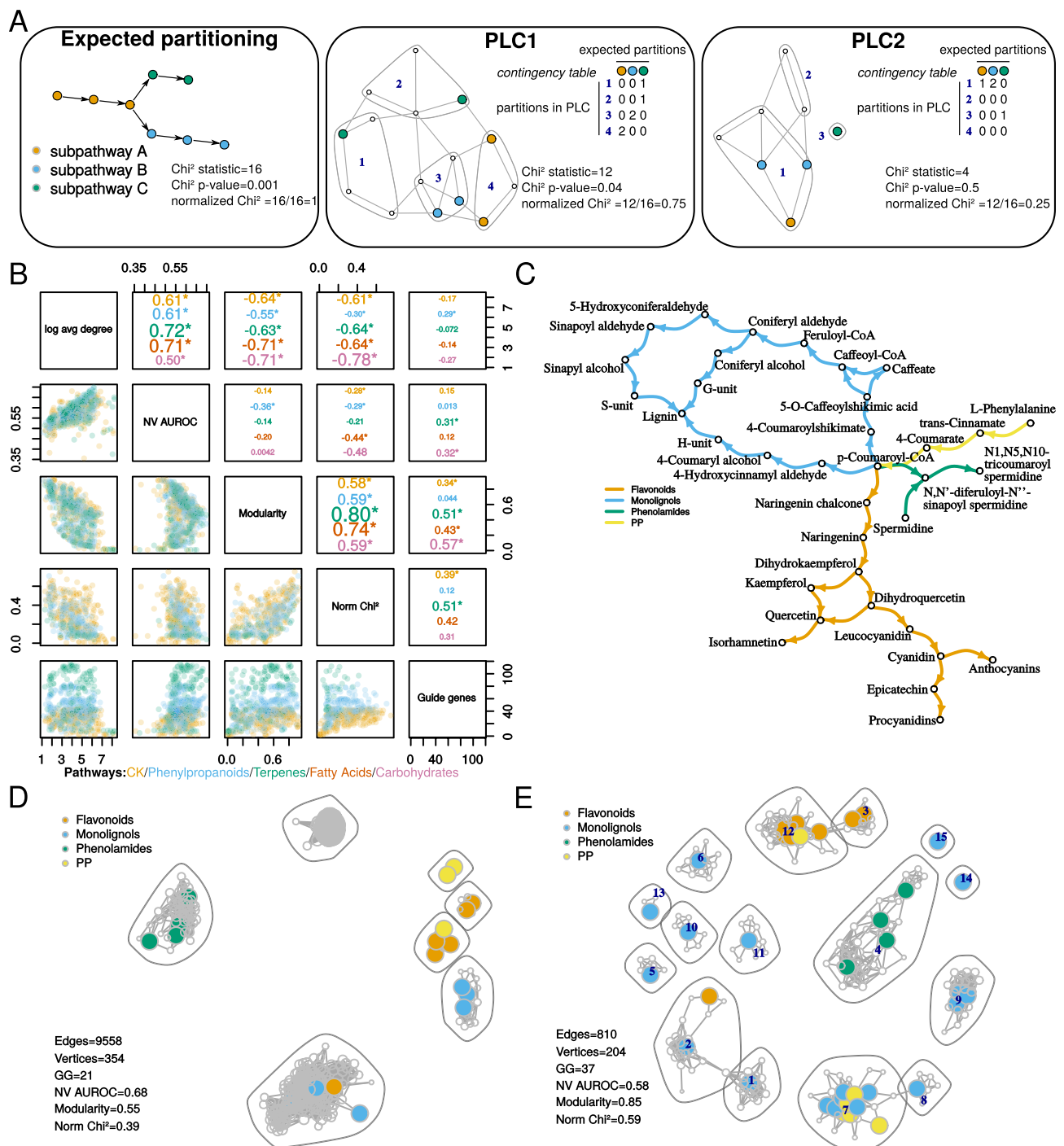


Figure 5. Trade-off in PLC subnetworks between performance in GO term recovery and partitioning guide genes into expected communities. **(A)** Example showing normalized Chi² statistic and *p*-value calculations comparing guide gene distribution into PLC communities (numbers in deep blue within polygons) to the expected partitioning (left; 3 subpathways). Two PLCs (one with a good partitioning (center); one with a weak partitioning (right)) are shown here but the contingency matrix used in Chi² calculations is described for only one of them (center). **(B)** Pair plot showing correlations (Spearman's rho, asterisks show significance *p* < 0.001, upper panel) and scatterplots (lower panel) between average network node degree, NV AUROC, normalized Chi², modularity and the number of guide genes in the network. Each point in the lower panels (scatterplots) represent one network for which 2 characteristics (eg NV AUROC and modularity) are compared. Data are presented for each pathway separately with a specific color. **(C)** The expected partitioning of phenylpropanoid related guide genes was compared to two PLC: **(D)** higher predictability and lower modularity (microarrays raw PCC) and **(E)** lower predictability and higher modularity (microarrays PCC-HRR). In **(D)** and **(E)**, colored vertices correspond to genes encoding enzymes catalyzing steps of similar color in **(C)**. Community (surrounded by grey polygons) numbers in **(E)** are indicated in deep blue and can be used to access Supplementary Table 3.

Pathway	Genes	Number of subpathways	Subpathway names (KEGG module accession)
Phenylpropanoids	43	4	core phenylpropanoid (PP), flavonoids, monolignols, phenolamides
Fatty acid	97	6	fatty acid biosynthesis (initiation (M00082), elongation (M00083), its ER-localized part (M00415)), jasmonic acid phytohormone biosynthesis (M00113) and β -oxidation (M00086 and M00087)
Carbohydrate	202	8	glycolysis (Embden-Meyerhof pathway (M00001) and the core module involving three-carbon compounds (M00002)), neoglucogenesis (M00003), pyruvate oxidation (M00307), citrate cycle (M00010), pentose phosphate pathway (M00004, M00006 and M00007)
Terpenes	64	6	mevalonate (M00095), methylerythritol (M00096), C10-C20 isoprenoid (M00366), beta-carotene (M00097), abscisic acid hormone (M00372) and phytosterol (M00371) biosynthetic blocks
Cytokinin signaling	37	?	?

Table 1. Pathway description. ?Indicates that partition in sub-pathway is not known.

normalized Chi^2 ($\rho > 0.59$, $p < 0.001$). We found that PLC performance (NV AUROC) was almost negatively correlated with normalized Chi^2 ($\rho < -0.2$) indicating that guide genes were clustered correctly at the expense of capturing GO associated gene pairs. Given the CK pathway structure, partitioning based on protein functions (receptor, transducer or response regulator) did not result in high Chi^2 values, suggesting that partitions in the co-expression networks contained guide genes from different levels, reinforcing the existence of specific sub-pathways. These results indicated a trade-off in PLC between edge quality and guide gene partitioning. A visual examination of PLC with either lower modularity and higher NV AUROC (Fig. 5D) or higher modularity and lower NV AUROC (Fig. 5E) revealed that PLC with higher modularity as well as higher Chi^2 values displayed a biologically relevant organization. Such subgraphs had generally a lower average node degree and a higher representation of guide genes rendering their analysis more convenient. Taking the phenylpropanoid pathway as an example, the PCC-HRR based TPM network (Fig. 5E, with a higher modularity) correctly clustered genes from the core phenylpropanoid (PP) and the flavonoid modules while the raw PCC network did not (Fig. 5D, with a higher NV AUROC). Similar results were observed with the four other pathways with either microarray or RNA-seq datasets (Supplementary Fig. 3). Modularity and normalized Chi^2 could therefore be considered as consistent quality metrics for PLC. NV AUROC should also be considered to ensure that subgraphs had a minimum predictability (>0.55).

HRR-CCs optimize recovery and clustering of guide genes in PLC. The best performing dataset \times distance measurement combinations were searched by analyzing NV AUROC, modularity and normalized Chi^2 among networks with a Chi^2 $p < 0.05$. Statistical effects of dataset, distance, ranking and their interactions on subgraph characteristics were analyzed by ANOVA for each pathway. Ranking and distance measurements had generally the strongest effects on modularity and normalized Chi^2 ($p < 2e-5$) (Fig. 6A,B). Ranking had a significant effect on NV AUROC ($p < 0.01$) but was weaker than distance measurement ($p < 1e-4$). Datasets only had a significant effect on modularity ($p < 0.002$). Significant interactions were rarely observed between these three factors (*i.e.* in few pathways and with a weak effect). This revealed that the different RNA-seq normalizations had only minor effects on these PLCs. Taken as a whole, networks obtained with raw datasets had a significant higher NV AUROC (t-test, mean in raw = 0.58, mean in HRR = 0.57, $p < 0.01$) but significant lower modularity (mean in raw = 0.35, mean in HRR = 0.68, $p < 2.2e-16$) and lower normalized Chi^2 value (mean in raw = 0.20, mean in HRR = 0.35, $p < 2.2e-16$) (Fig. 6A). It therefore appeared that clustering guide genes correctly was improved with CC ranked with HRR at the expense of performance. NV AUROCs in HRR-based networks were generally higher than 0.55, indicating an average low performance in GO capture (Fig. 6A). In non-ranked distances, PC resulted in the weakest NV AUROC, while MI and raw SCC based networks displayed the highest NV AUROC (Fig. 6B). This weakness in PC based networks was compensated neither by a higher modularity nor by a higher normalized Chi^2 statistic.

A more detailed examination of best PLC subgraphs maximizing either modularity or NV AUROC, revealed that each of the five pathways involved specific dataset \times distance measurement combinations. PCC-HRR based networks were always found to maximize modularity (Fig. 6C) and normalized Chi^2 (Fig. 6D) with almost all datasets. Raw distance based PLCs had a higher NV AUROC and some of them also had a good modularity but they also had a lower normalized Chi^2 statistic indicating they contained fewer guide genes (*e.g.* raw RNA-seq counts with raw SCC in the terpene PLC). The results suggest that PCC-HRR could be used as a reliable distance measurement whatever the dataset. Careful analysis of PLC obtained from PCC-HRR revealed the presence of relevant associations in each PLC (Supplementary Fig. 3 and Table 3). For example, community 12 from the phenylpropanoid PLC obtained with microarray data processes with PCC-HRR (Fig. 5D) contained AT1G06000 encoding a Flavonol 7-O-rhamnosyltransferase and was clearly associated with other genes from the flavonoid sub-pathway. This gene was not detected in the raw PCC PLC (Fig. 5C). Other examples are highlighted in yellow in Supplementary Table 3.

Vertex and edge co-occurrence in microarray and RNA-seq based PLC subgraphs. Edge co-occurrence in networks constructed from expression datasets obtained by different technologies may be considered as a further validation. Quantifying gene expression with microarrays relies on probe hybridization by sequence complementary while with RNA-seq, short reads are mapped back *in silico* to the reference transcriptome. The two main differences

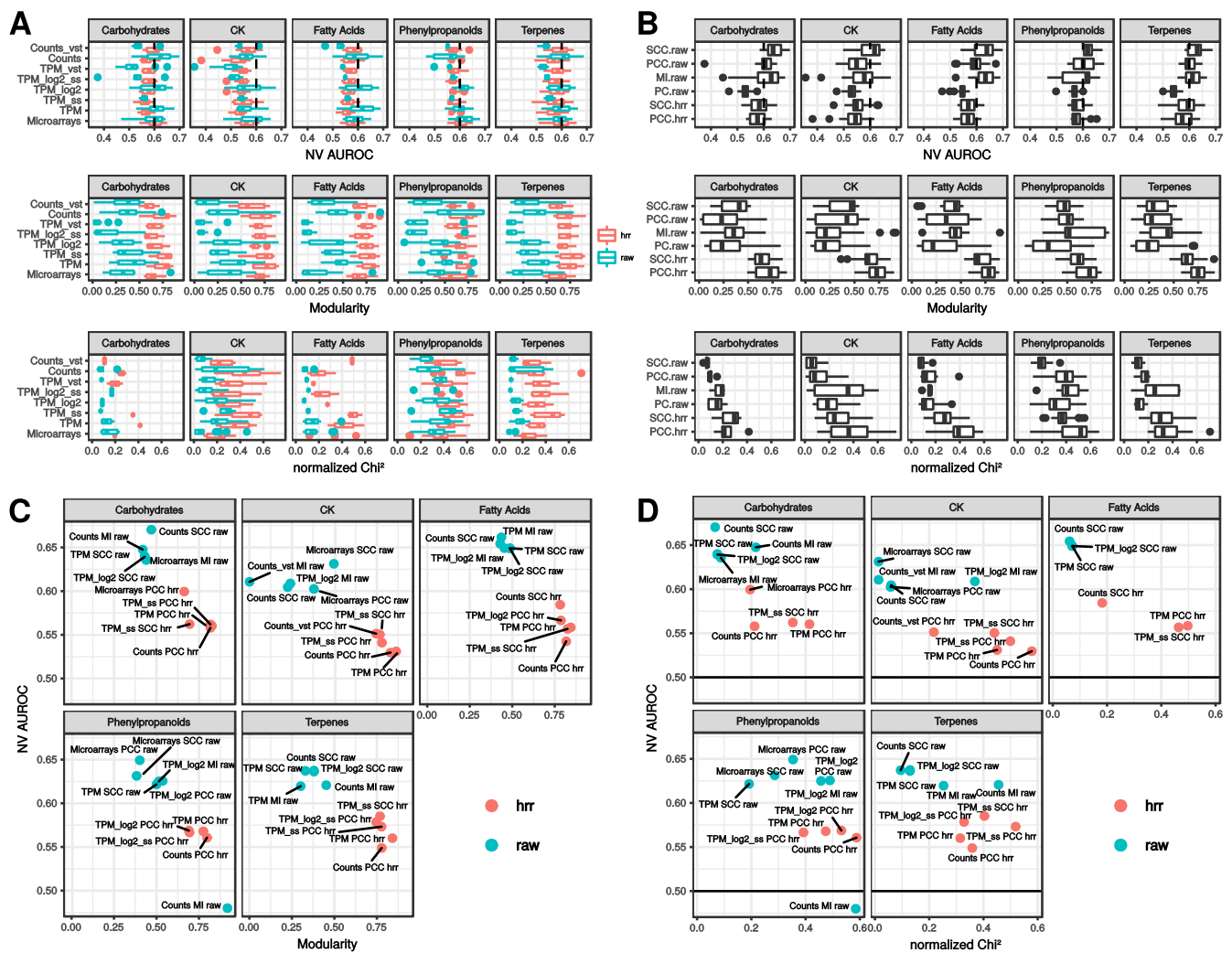


Figure 6. PLC subnetwork performance. Performance in capturing GO terms (NV AUROC), modularity and normalized χ^2 value distribution in interactions between datasets and ranking methods (A) and between distance measurement and ranking methods (B) showing the dominant effect of the ranking procedure (raw vs HRR) on these metrics. (C) Modularity and NV AUROC of the five top NV AUROC networks and 5 top modularity networks. (D) Normalized χ^2 statistic and NV AUROC for the same networks.

between these technologies are (i) the number of quantified transcripts (due to the completion of genome annotation) and (ii) the dynamic range (fluorescent probe intensities for microarrays, *in silico* read counts for RNA-seq). Because microarrays and RNA-seq technologies differ, edges co-occurring in networks obtained from these two technologies are probably more relevant. In Fig. 4C, we analyzed co-occurrence in global networks and found that HRR ranked CCs apparently increased the number of co-occurring edges between microarrays and RNA-seq. To get more insights into co-occurrence in PLCs, common edges and vertices were counted in pairwise intersections of networks (RNA-seq vs microarrays) obtained with the six distance measurements and set at a 1,000 vertices. The resulting intersection networks were further characterized by the number of represented guide genes, their normalized χ^2 statistic, modularity and NV AUROC. This evaluation was performed with the RNA-seq dataset expressed as TPM only because we showed in the previous section that normalization methods had a minor impact on PLC. In addition, TPM networks with raw distance methods had enough vertices to correctly extract PLC (it was not the case with raw distances, e.g. for TPM normalized with VST as revealed by their very low normalized χ^2 statistics; Fig. 6A).

Many more co-occurring edges were generally recovered when raw CC and MI networks were compared (e.g. 18,334 averaged over the five pathways with MI networks vs 550 with PCC-HRR networks; Supplementary Fig. 4). At a 1,000 vertices, all raw networks but PC contained more edges (221,297 and 85,059 in average for microarrays and TPM) than HRR-CCs networks (12,431 and 12,877). This might have resulted in more co-occurrences between MI networks. PC networks had the lowest number of co-occurring vertices (94 in average) but intersections from MI and/or raw CC had comparable vertex number (268) to intersection networks from CC-HRR (267 in average) (Supplementary Fig. 4). These results suggest that HRR-based networks have strong overlaps. Intersections of PCC-HRR subgraphs were able to maximize the % of guide genes (mean of 75% over the 5 PLC),

modularity (0.78) and normalized Chi² statistic (0.70) (Fig. 7). Detailed characteristics for each PLC are presented in Supplementary Fig. 4. Modularity was generally high in the intersection between CC-HRR networks (>0.70) but intersections with SCC-HRR displayed lower normalized Chi² values (<0.6). Intersection network performance in recovering GO terms was globally low (Fig. 7D). The highest NV AUROCs were observed in intersections between MI networks (0.52), MI (microarrays)–raw SCC (TPM)(0.54) and raw PCC (microarrays)–raw SCC (TPM)(0.52) (Fig. 7D). Intersection networks and their contents are available in Supplementary Fig. 5 and Supplementary Table 4. Again, we found candidate genes not included in the guide gene sets that were correctly associated with other guide genes (highlighted in yellow in Supplementary Table 4). Taking the phenylpropanoid pathway as an example, Fig. 7E shows edge and vertex co-occurrence between MI networks and Fig. 7F between PCC-HRR networks. The co-occurrence network obtained from MI contained fewer guide genes (26 vs 41) and displayed lower modularity (0.49 vs 0.67) and normalized Chi² statistic (0.39 vs 0.66). Although it had a higher NV AUROC (0.6 vs 0.46), its structure did not reflect that of the expected pathway (Fig. 5C). For example, phenolamide related genes were not represented. Average guide gene degree (33) was below the average degree of the remaining nodes (100) indicating that guide genes were only slightly connected to other genes in this co-occurrence network from MI PLC. By contrast, guide gene degree (11.4) was very similar to the other node degree (11.1) revealing an uniform integration of guide genes with other genes in the co-occurrence network of PCC-HRR PLCs. As observed in co-occurrence in large networks (Fig. 4B), RNA-seq TPM normalized with VST had slightly more edges in common with microarray networks. We therefore compared PCC-HRR PLC between microarrays and RNA-seq TPM normalized with VST. Intersection networks had very similar characteristics to that observed between microarrays and RNA-seq TPM. Although it contained slightly more co-occurring vertices and edges in average (360 and 1,252 respectively with TPM VST vs 240 and 550 with TPM), it displayed fewer guide genes (54 vs 57). TPM normalized with VST could therefore be an interesting alternative to TPM. PLC intersection networks and their description are available in Supplementary Fig. 6 and Table 5.

Discussion

Pathway Level-Correlation (PLC) is an interesting approach to capture biologically relevant transcriptional relationships using guide genes (e.g. genes involved in a same metabolic pathway) from transcriptome-wide co-expression networks. Our present work highlights that distances between genes calculated with highest reciprocally ranked PCC (PCC-HRR) improve PLC. The main improvement was guide gene representation. PCC-HRR based PLCs contained more guide genes than observed with other distances and they were generally more correctly partitioned into expected sub-pathways in the co-expression network. This was associated with a lower mean node degree and a higher modularity but also with a slightly weaker performance in GO term recovery. Our results propose that modularity and normalized Chi² values could be used as reliable indicators of PLC quality. We also observed that edge and vertex co-occurrences in PLCs obtained with PCC-HRR and microarray and RNA-seq TPM data can be used to construct relevant networks. A surprising observation was that in our conditions, for most combinations tested, true positive rates remained higher than false positive rates in spite of increasing network sizes. A similar trend using small *E. coli* and *S. cerevisiae* networks (<110 nodes) has been previously observed with CCs⁸. However increasing network sizes inherently increases the number of false positive associations and it is clear that TPR is likely to increase at a slower rate than FPR above a given threshold. Thresholding is a very complex procedure which deeply impact network topology (Couto *et al.* 2017). The user should probably focus on a threshold that maximizes GO term capture while keeping the total number of edges as low as possible to avoid too strong an increase in FPR. The resulting FP which may have different origins: (i) true FP corresponding to apparent direct associations between two genes because they are both more correlated to a third gene (as exemplified in De la Fuente *et al.* 2004) or (ii) yet unknown true associations. In all cases, functional experimentation is required to validate or reject an association. This suggests that co-expression studies should test different confidence thresholds to efficiently capture gene associations. Evaluating network quality was done in respect of the Arabidopsis reference GO annotation set. We found that the NV AUROC¹⁹ evaluates networks efficiently and was generally in accordance with significantly enriched GO term counts and TPR vs FPR curves. NV AUROC has the advantage of being a more global measure of predictability (values above 0.6 can be considered as moderate). Different distance measurements displayed different efficiencies according to the dataset but as a general trend, performance of the different combinations were similar (e.g. between microarrays and RNA-seq TPM in Fig. 3B). The same performance was obtained for different topologies: high node degree (more edges and fewer vertices) for MI and raw CC networks vs lower node degree (fewer edges and more vertices) for CC-HRR networks. PC networks displayed a high performance with microarray data only, suggesting that PCs calculated with ‘corpcor’ R package may not be recommended for RNA-seq data. A recent study has focused on metabolic pathways in plants using mutual ranks, another CC ranking method¹⁶. Complementary to this previous work, we found that ranking CCs increases vertex number without penalizing absolute network performance. Contrastingly, an opposite trend was observed in another study³¹, where larger networks displayed a lower Matthew Coefficient when compared to protein-protein interactions or regulatory networks. This indicates that different absolute performance measurements lead to different results and interpretations but this might also be due to our datasets which were larger than theirs. Another advantage of CC-HRR was that it clearly homogenized network characteristics from differently normalized RNA-seq datasets in addition to increase the number of co-occurring edges between microarrays and RNA-seq. The improved performance of HRR may be explained by its ability to integrate the whole transcriptional landscape of each gene thanks to the reciprocal rank calculation. In addition to normalize biases observed in raw CC values when using different data normalization procedures¹⁵, it probably added robustness to correlations because a low HRR value for a gene pair is observed only if the two genes had no higher correlations with other genes and this probably correct for noise in the expression dataset.

As revealed recently³², highlighting correlations between genes may require specific data processing or distance algorithms best suited to their query pathway. We also found that each of the five PLCs performed best

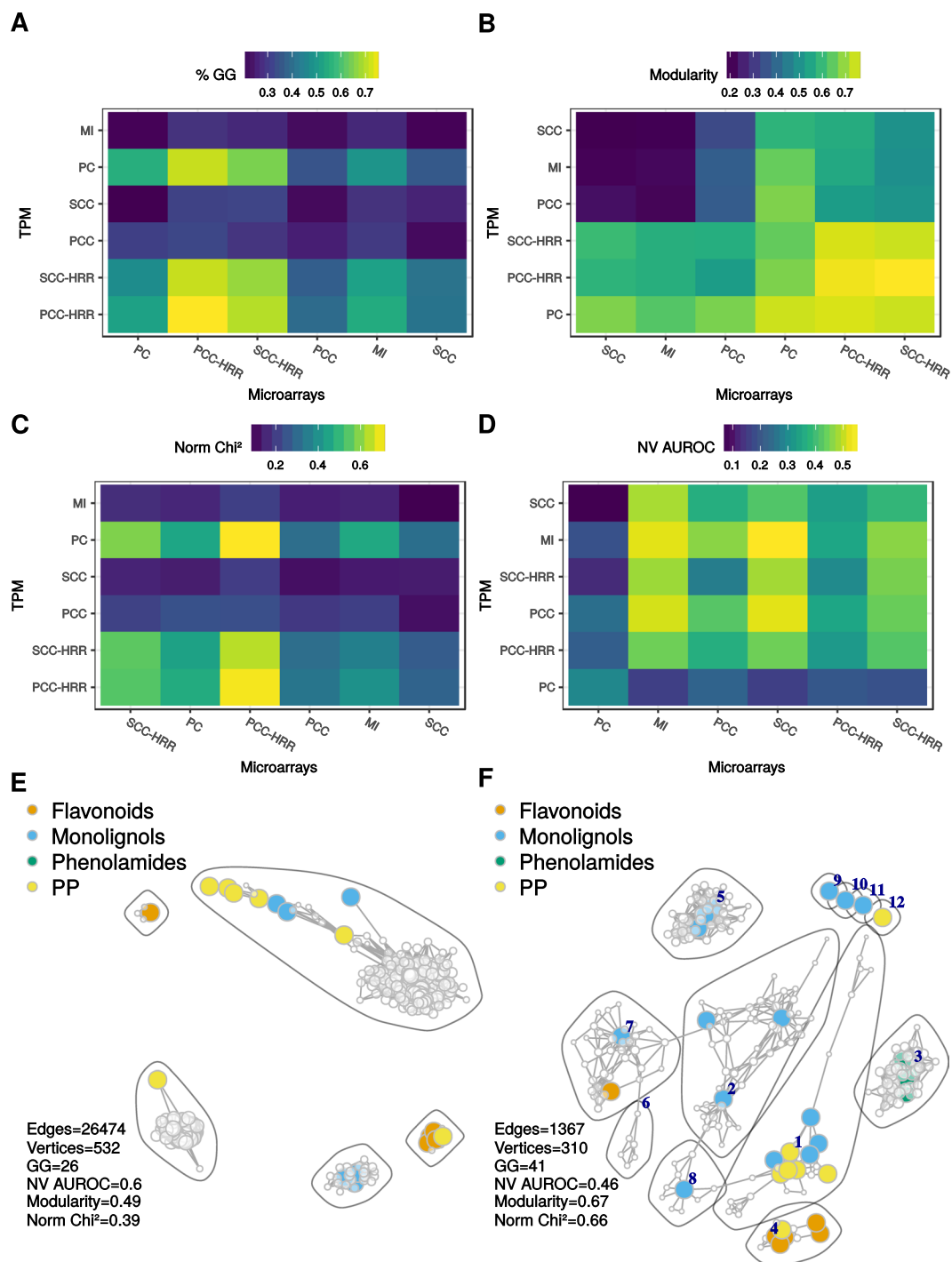


Figure 7. Characteristics of co-occurrence networks between microarrays and RNA-seq TPM. Percentage of guide genes (GG; **A**), modularity (**B**), normalized Chi² statistic (agreement with guide gene partitioning, **C**) and NV AUROC (GO term performance, **D**) were averaged over the 5 PLCs. Labels are ordered according to a hierarchical clustering. Co-occurrence networks obtained from phenylpropanoid PLC obtained with MI (**E**) or PCC-HRR (**F**). GG corresponds to guide gene number in the networks. Community numbers in **F** are indicated in deep blue and can be used to access Supplementary Table 4.

with specific RNA-seq normalizations (Fig. 6C,D) but RNA-seq TPM processed with PCC-HRR always provided informative networks which can be used as reliable starting point because they matched well expected pathway structure. In our case, the different data normalizations had a relatively weak effect on PLC characteristics especially when CCs were used with HRR. In a comparative analysis³¹, the authors have shown that PCC networks from VST normalized counts were more comparable to those from microarrays. In our case, VST normalization slightly improved the overlap between RNA-seq TPM and microarrays both at the global and targeted levels. This normalization can thus be further considered for co-expression studies. A fast greedy approach maximizing

modularity was used to detect communities within PLC subgraphs. Guide gene partitioning in these communities was compared to expected partitions in subpathways with a normalized χ^2 test (Fig. 5A). We found that correct guide gene partitioning was negatively correlated with NV AUROCs but positively with modularity. Subnetworks with highest NV AUROCs but lower modularity such as those obtained with MI represented fewer guide genes and displayed large edge numbers. In these networks, guide genes formed inappropriate structures (Supplementary Fig. 5). We applied PLC to five pathways varying in size and nature. For the four metabolic pathways, PLC extracted from PCC-HRR based networks were able to cluster guide genes in the proper subpathways (Supplementary Fig. 5). Guide genes were associated in communities resembling subpathways and containing genes not included in the query gene set but known to be involved with the given pathway or being good candidates to be functionally validated (Supplementary Table 4). A similar PLC approach has been recently performed¹⁶ using the Arabidopsis aliphatic glucosinolate pathway. In this previous work, the authors have successfully reconstructed this pathway and identified a new candidate glucosyltransferase that could be part of it. This demonstrated again that PLC is a powerful approach to complete biological pathways. When tested with a signaling pathway, we found that PLCs also displayed meaningful communities. For example, the CK signaling pathway is physiologically well known but its organization at the molecular level is far from being understood²⁸. In particular, it is unclear how multi-family members of each signaling level (receptor, transducer and response regulator) interact with each other to drive a specific physiological response. In the PLC dedicated to the CK signaling pathway, PCC-HRR with microarrays suggested preferential transcriptional associations that have been described in the literature³³. For example AHP2, AHP3 and AHP5 were grouped in the same module (module 7 Supplementary Fig. 5 and Table 4). These three AHPs have been reported to negatively regulate tolerance to abiotic stress³⁴. The same community also contained AHK3, ARR1 and ARR2. Those three members are known to regulate primary root meristem activity and senescence³⁵. AHK4, AHK2 and ARR14 which have been shown to regulate shoot apical meristem activity were grouped in the same community³⁴. In addition, we saw clear associations between ETR1 and AHK3 in individual PLC subgraphs. Such association highlights crosstalk already known between CK and ethylene signaling pathways²⁹. The co-occurrence pathway was relatively sparse in contrast to the metabolic pathways (Supplementary Fig. 5). It is possible that vertex number for this analysis (1,000) might have been too small to capture complex associations within this signaling pathway. Using VST normalized TPM increased edge and vertex number in the co-occurrence network (Supplementary Fig. 6 and Table 5). The above-described associations were also found in this co-occurrence network. While effective in revealing strong gene associations, merging PLC from microarray and RNA-seq data could miss other relevant associations. First, experimental conditions represented by each starting dataset are not completely overlapping. Together with inherent differences due to dynamic range, this leads to networks with very different edge compositions and node degrees¹⁹, explaining the relative weak overlap between networks. Second, RNA-seq expression data include genes that are not included in the GPL198 microarray. As an example, some important genes in aliphatic glucosinolate biosynthesis were not represented in a previous Arabidopsis microarray dataset but found in RNA-seq expression matrices from other related species¹⁶.

To capture transcriptional environment of a query gene list, distance calculations have to be performed on the whole transcriptome. Calculating partial correlations was particularly challenging but using a covariance shrinkage estimator worked well in terms of computing performance. It took less than 2 h for RNA-seq expression matrices but more than 12 h for the microarray dataset. By contrast, our program which is freely available at (<https://github.com/EA2106-Universite-Francois-Rabelais/Expression-network-analysis>) was able to calculate PCC-HRR in less than 3 h for both datasets. As PCC-HRR resulted in relevant networks, this tool can be useful for further studies requiring many computations such as analyzing sample size impact on PLC or testing other normalization methods.

The present work demonstrates that Pearson's Correlation Coefficients (PCC) on which highest reciprocal ranking (HRR) was applied can be used to construct reliable global and targeted networks. When considering Pathway Level Correlation (PLC) with a set of guide genes, three reliable measures can be used for evaluation: NV AUROC as a global indicator of GO recovery (expecting values > 0.5), modularity (between 0 and 1, 1 being the best network partition) and normalized Chi statistic (between 0 and 1, 1 indicating a perfect match with an expected partition). Clustering guide genes correctly was at the expense of capturing GO terms and dataset \times distance measurement combination should be carefully selected to construct reliable PLC. Although specific RNA-seq data normalizations may be adapted to each pathway of interest, using TPM with PCC-HRR generated accurate and safe PLC. Using PCC with HRR also increased the quality of co-occurrence networks between RNA-seq and microarrays.

Methods

Microarray data preparation. Experiment accessions (GSE) for GPL198 (Arabidopsis ATH1, 22,746 genes) were retrieved from ArrayExpress (Supplementary Table 6). Signal intensities per probe were generated with R³⁶ using the 'arrayexpress' package³⁵. The function 'getAE' was used to convert the raw signal CEL files. Array normalization was performed per GSE using the 'justRMA' function of the 'affy' package. This procedure applies a background correction together with a quantile normalization to correct for biases within arrays and finally returns log₂-transformed corrected signal intensities. All 10,095 arrays were combined into a single file and subjected to a quality control based on upper quartile dispersion (75%) and Kolmogorov-Smirnov statistical testing for outliers using an empirical cumulative distribution function as described previously³⁷. A total of 142 arrays were considered outliers in the two tests and discarded from the final matrix. Each array was finally centered and scaled individually.

RNA-seq data preparation. 2,549 RNA-seq accessions obtained for *A. thaliana* were retrieved from ArrayExpress. Fastq files were obtained from the SRA after converting.sra files with the SRA ToolKit function

'fastq-dump' with the `-split-files` option for paired-end sequencing runs. Reads were systematically trimmed with Trimmomatic using adapter files according to the Illumina platform used for the runs³⁸. Trimmed reads were pseudo-aligned to predicted transcripts from the representative gene models of Arabidopsis TAIR genome v10 (33,604 transcripts) with Salmon v0.7.2 using the variational Bayesian EM algorithm mode to improve abundance estimation³⁹. Only samples displaying a mapping rate of reads >30% were kept, resulting in a final matrix containing 1,676 samples (Supplementary Table 6). RNA-seq counts were used as non-normalized raw counts or expressed as Transcript per Million to correct for sequencing depth. Normalization by Variance Stabilizing Transformation (VST) was performed with the DESeq2 R package. This normalization method aims at limiting the variance dependence to the mean⁴⁰.

Distance calculations. Before calculations, zero-variance genes were discarded. CCs (Pearson or Spearman) are computationally intensive particularly in the case of large matrices. Highest Reciprocal Ranking (HRR) of CCs for genes A and B is calculated as $\max(\text{rank}(\text{CC}(A,B)), \text{rank}(\text{CC}(B,A)))$. For each gene, all CC values are first transformed as ranks, with 0 corresponding to the gene rank against itself. Ranks are subsequently compared and the highest value is retained for each gene pair. We developed a tool written in C allowing the easy parallelization of these computations. Briefly, for a given initial matrix containing n genes and p samples, the number of cores c allocated is used to split the dataset into n/c submatrices. In case of non-integer value, the last line of the matrix is replicated (without incidence on PCC or rank values) so that n/c is an integer. PCC or HRR are then calculated for each gene pair using communication between CPUs with Message Passing Interface. The program delivers c files containing $n/c \times n$ values corresponding to PCC or HRR. This program is freely available on Github (<https://github.com/EA2106-Universite-Francois-Rabelais/Expression-network-analysis>). To calculate SCCs, expression values were first ranked in R. Mutual information (MI) which is reported to better capture non linear relationships⁹ were calculated with the 'knni.all' function of the Parmigene R package⁴¹. This function estimates MI using a k -nearest neighbor. Partial correlations were challenging to compute on genome scale expression matrices. Partial correlations are usually calculated from multiple linear regressions or by inverting the correlation matrix and used in Graphical Gaussian Models⁴². Our expression matrices had many more variables (genes) than samples therefore regression methods would have required a Lasso or Ridge penalization to estimate coefficients. However, this procedure generally leads to memory errors when considering more than 30,000 variables. We found that the most computationally appropriate method in our case was to estimate shrinkages of partial correlations with the R package 'corpcor' (<http://strimmerlab.org/software/corpcor/>). This package is maintained by Korbinian Strimmer's team^{43,44}. We used 'pcor.shrink' function which relies on the inversion of the shrunken estimated covariance matrix to estimate partial correlations and which is suited for matrices with more genes than samples.

Reference dataset. We used the Arabidopsis Gene Ontology (GO) standard dataset to assess network quality. The annotation file provided by the AGRIGO database⁴⁵ and was filtered out to remove all terms with a IEA evidence code and keep only functionally attributed terms. We also removed GO terms represented by less than 5 genes or more than 100 to remove non-specific terms.

Global Network analysis. **Construction:** For each dataset \times distance combination, we dynamically set a threshold to obtain arbitrary lists of 10 million best gene pairs (with CC above or HRR below that threshold), *i.e.* less than 2% of the total possible edges. Networks were then constructed with the 1, 5, 10, 20, 40, 60 or 80% best pairs from these lists. Thresholds used to get the 10 million gene pairs are reported in Table S2. Global networks were analyzed as adjacency matrices in R. **Network characteristics:** besides classical topological characteristics such as vertex and edge numbers and mean node degree (the average number of connections for each vertex), we evaluated network quality by comparison with the reference dataset (Fig. 2). In a first approach, we built a confusion matrix by classifying edges as false or true positives, considering edges as valid if both genes were annotated with at least one same GO term. In this confusion matrix, true positives (TP) corresponded to gene pairs also found in the GO annotation, false positive (FP) to genes associated in the network but not in the GO annotation, false negatives (FN) to pairs in the GO annotation not predicted in the network and finally true negatives (TN) genes pairs not predicted in the network and the annotation table. This confusion matrix was used to calculate True Positive Rates (TPR) and False Positive Rates (FPR). TPR and FPR were obtained at various confidence thresholds (*i.e.* for networks differing in sizes) and used to draw a TPR vs FPR curve as described elsewhere¹⁵. These curves were only partial because we included only the first 10 million best pairs. This was useful to pinpoint the importance of low FPR⁴⁶. In the second and third approaches, we relied on the guilt-by-association principle to estimate network predictability. In the second method, we used the 'predictions' function of EGAD R package⁴⁷. For each gene, this function counts the number of connected genes annotated with an identical GO term and divides this count by the gene's degree. These scores are next ordered decreasingly to construct a TPR vs FPR curve for each network. It differs from the first approach described above because here TPR and FPR are not obtained from different confidence thresholds (and from different networks) but from all possible true positive and false positive edges in the current network. A global Area Under Receiver Operating Characteristic (global AUROC) was calculated from each of these TPR/FPR curves. In the third method, predictability was evaluated using a neighbor voting (NV) algorithm. In this case, an AUROC is calculated for each GO term from the ability of genes to predict the GO annotation of their direct neighbors in a 3-fold cross-validation^{19,48}. A mean NV AUROC was calculated for each network. In addition to ROC analysis, we counted GO terms that were significantly enriched with gene pairs using a hypergeometric test with R.

Pathway Level Correlation. **Construction:** In PLC, subnetworks were constructed from global networks (see above) by keeping edges connecting at least one guide gene. Guide gene lists are indicated in Supplementary

Table 2. The R package ‘igraph’⁴⁹ v1.0.1 was used to construct and visualize these targeted networks with a force-directed layout (Fruchterman-Reingold). **Community Detection:** Modules containing densely connected vertices were estimated within each network by using a fast greedy approach which aims at maximizing modularity of the detected communities³⁰. Modularity measures how good a network partition is by calculating for each gene the number of edges within its community against its total node degree. The fast greedy approach optimizes modularity over all possible divisions of the network and has been shown to perform well on large networks. Guide genes clustering within the communities was compared to expected partitions in sub-pathway with a Pearson’s Chi² test and Monte-Carlo simulated *p*-values with 2,000 replicates. This test was based on a contingency table with dimensions $n \times m$ (n , sub-pathway number, m community number in the co-expression network) and each entry corresponding to the number of genes being in communities n_i and m_j , with $i = 1$ to n and $j = 1$ to m . Because Chi² statistic depends on sample number, values were normalized by dividing them to the maximal expected value (the ideal partition) of each pathway. This resulted in a score ranging from 0 to 1, 0 being a random distribution of guide genes in the network and 1 to the exact partitioning.

Data availability. All datasets generated during and/or analyzed during the current study are available from the corresponding author on reasonable request.

References

1. Oliver, S. Proteomics: guilt-by-association goes global. *Nature* **403**, 601–603 (2000).
2. Lisso, J., Steinhäuser, D., Altmann, T., Kopka, J. & Müssig, C. Identification of brassinosteroid-related genes by means of transcript co-response analyses. *Nucleic Acids Research* **33**, 2685–2696 (2005).
3. Wei, H. *et al.* Transcriptional coordination of the metabolic network in arabidopsis. *Plant physiology* **142**, 762–774 (2006).
4. Ruiz-Sola, M. Á. *et al.* Arabidopsis geranylgeranyl diphosphate synthase 11 is a hub isozyme required for the production of most photosynthesis-related isoprenoids. *New Phytologist* **209**, 252–264 (2016).
5. Guerin, C. *et al.* Gene coexpression network analysis of oil biosynthesis in an interspecific backcross of oil palm. *The Plant Journal* **87**, 423–441 (2016).
6. Coman, D., Rütimann, P. & Gruijssem, W. A flexible protocol for targeted gene co-expression network analysis. *Plant Isoprenoids: Methods and Protocols* 285–299 (2014).
7. Caputi, L. *et al.* Missing enzymes in the biosynthesis of the anticancer drug vinblastine in madagascar periwinkle. *Science* <https://doi.org/10.1126/science.aat4100> (2018).
8. Maetschke, S. R., Madhamshettiwar, P. B., Davis, M. J. & Ragan, M. A. Supervised, semi-supervised and unsupervised inference of gene regulatory networks. *Briefings in bioinformatics* **15**, 195–211 (2013).
9. de Siqueira Santos, S., Takahashi, D. Y., Nakata, A. & Fujita, A. A comparative study of statistical methods used to identify dependencies between gene expression signals. *Briefings in bioinformatics* **15**, 906–918 (2013).
10. De La Fuente, A., Bing, N., Hoeschele, I. & Mendes, P. Discovery of meaningful associations in genomic data using partial correlation coefficients. *Bioinformatics* **20**, 3565–3574 (2004).
11. Li, Y., Pearl, S. A. & Jackson, S. A. Gene networks in plant biology: approaches in reconstruction and analysis. *Trends in plant science* **20**, 664–675 (2015).
12. Serin, E. A., Nijveen, H., Hilhorst, H. W. & Ligterink, W. Learning from co-expression networks: possibilities and challenges. *Frontiers in plant science* **7** (2016).
13. Blasi, M. F. *et al.* A recursive network approach can identify constitutive regulatory circuits in gene expression data. *Physica A: Statistical Mechanics and its Applications* **348**, 349–370 (2005).
14. Chai, L. E. *et al.* A review on the computational approaches for gene regulatory network construction. *Computers in biology and medicine* **48**, 55–65 (2014).
15. Obayashi, T. & Kinoshita, K. Rank of correlation coefficient as a comparable measure for biological significance of gene coexpression. *DNA research* **16**, 249–260 (2009).
16. Wisecaver, J. H. *et al.* A global co-expression network approach for connecting genes to specialized metabolic pathways in plants. *The Plant Cell Online tpc-00009* (2017).
17. Mutwil, M. *et al.* Assembly of an interactive correlation network for the arabidopsis genome using a novel heuristic clustering algorithm. *Plant Physiology* **152**, 29–43 (2010).
18. Tsuchiya, M., Giuliani, A., Hashimoto, M., Erenpreisa, J. & Yoshikawa, K. Self-organizing global gene expression regulated through criticality: mechanism of the cell-fate change. *PLoS one* **11**, e0167912 (2016).
19. Ballouz, S., Verleyen, W. & Gillis, J. Guidance for rna-seq co-expression network construction and analysis: safety in numbers. *Bioinformatics* **31**, 2123–2130 (2015).
20. Song, L., Langfelder, P. & Horvath, S. Comparison of co-expression measures: mutual information, correlation, and model based indices. *BMC bioinformatics* **13**, 328 (2012).
21. Censi, F., Giuliani, A., Bartolini, P. & Calcagnini, G. A multiscale graph theoretical approach to gene regulation networks: a case study in atrial fibrillation. *IEEE Transactions on Biomedical Engineering* **58**, 2943–2946 (2011).
22. Huang, S. Reprogramming cell fates: reconciling rarity with robustness. *Bioessays* **31**, 546–560 (2009).
23. Besseau, S. *et al.* Flavonoid accumulation in arabidopsis repressed in lignin synthesis affects auxin transport and plant growth. *The Plant Cell* **19**, 148–162 (2007).
24. Zhang, Y. *et al.* Phenolic compositions and antioxidant capacities of chinese wild mandarin (citrus reticulata blanco) fruits. *Food chemistry* **145**, 674–680 (2014).
25. Winkel-Shirley, B. Flavonoid biosynthesis. A colorful model for genetics, biochemistry, cell biology, and biotechnology. *Plant physiology* **126**, 485–493 (2001).
26. Elejalde-Palmett, C. *et al.* Characterization of a spermidine hydroxycinnamoyltransferase in malus domestica highlights the evolutionary conservation of trihydroxycinnamoyl spermidines in pollen coat of core eudicotyledons. *Journal of experimental botany* **66**, 7271–7285 (2015).
27. Kanehisa, M., Sato, Y., Kawashima, M., Furumichi, M. & Tanabe, M. Kegg as a reference resource for gene and protein annotation. *Nucleic acids research* **44**, D457–D462 (2016).
28. Hwang, I., Sheen, J. & Müller, B. Cytokinin signaling networks. *Annual review of plant biology* **63**, 353–380 (2012).
29. Zdarska, M. *et al.* Illuminating light, cytokinin, and ethylene signalling crosstalk in plant development. *Journal of experimental botany* **66**, 4913–4931 (2015).
30. Clauset, A., Newman, M. E. & Moore, C. Finding community structure in very large networks. *Physical review E* **70**, 066111 (2004).
31. Giorgi, F. M., Del Fabbro, C. & Licausi, F. Comparative study of rna-seq and microarray-derived coexpression networks in arabidopsis thaliana. *Bioinformatics* **29**, 717–724 (2013).

32. Uygun, S., Peng, C., Lehti-Shiu, M. D., Last, R. L. & Shiu, S.-H. Utility and limitations of using gene expression data to identify functional associations. *PLoS computational biology* **12**, e1005244 (2016).
33. Jiang, L. *et al.* Strigolactones spatially influence lateral root development through the cytokinin signaling network. *Journal of experimental botany* **67**, 379–389 (2015).
34. Wang, L. & Chong, K. The essential role of cytokinin signaling in root apical meristem formation during somatic embryogenesis. *Frontiers in plant science* **6** (2015).
35. Kauffmann, A. *et al.* Importing arrayexpress datasets into r/bioconductor. *Bioinformatics* **25**, 2092–2094 (2009).
36. R Core Team, R: A Language and Environment for Statistical Computing, R Foundation for Statistical Computing, Vienna, Austria <http://www.R-project.org> (2018).
37. Felts, F. A., Ficklin, S. P., Gibson, S. M. & Smith, M. C. Maximizing capture of gene co-expression relationships through pre-clustering of input expression samples: an arabidopsis case study. *BMC systems biology* **7**, 44 (2013).
38. Bolger, A. M. *et al.* Trimmomatic: a flexible trimmer for Illumina sequence data. *Bioinformatics* **30**(15), 2114–2120 Oxford University Press (2014).
39. Patro, R., Duggal, G., Love, M. I., Irizarry, R. A. & Kingsford, C. Salmon provides fast and bias-aware quantification of transcript expression. *Nature Methods* **14**, 417–419 (2017).
40. Love, M. I., Huber, W. & Anders, S. Moderated estimation of fold change and dispersion for rna-seq data with deseq2. *Genome biology* **15**, 550 (2014).
41. Sales, G. & Romualdi, C. parmigene—parallel r package for mutual information estimation and gene network reconstruction. *Bioinformatics* **27**, 1876–1877 (2011).
42. López-Kleine, L., Leal, L. & López, C. Biostatistical approaches for the reconstruction of gene co-expression networks based on transcriptomic data. *Briefings in functional genomics* **12**, 457–467 (2013).
43. Schäfer, J. & Strimmer, K. Learning large-scale graphical gaussian models from genomic data. In *AIP Conference Proceedings*, vol. 776, 263–276 (AIP, 2005).
44. Schaefer, J., Opgen-Rhein, R. & Strimmer, K. Corpcor: efficient estimation of covariance and (partial) correlation. R package version 1.4.7 (2007).
45. Du, Z., Zhou, X., Ling, Y., Zhang, Z. & Su, Z. Agrigo: a go analysis toolkit for the agricultural community. *Nucleic acids research* **38**, W64–W70 (2010).
46. Schrynmackers, M., Küffner, R. & Geurts, P. On protocols and measures for the validation of supervised methods for the inference of biological networks. *Frontiers in genetics* **4** (2013).
47. Ballouz, S., Weber, M., Pavlidis, P. & Gillis, J. Eged: ultra-fast functional analysis of gene networks. *Bioinformatics* **33**, 612–614 (2016).
48. Gillis, J. & Pavlidis, P. The impact of multifunctional genes on “guilt by association” analysis. *PLoS one* **6**, e17258 (2011).
49. Csardi, G. & Nepusz, T. The igraph software package for complex network research. *InterJournal, Complex Systems* **1695**, 1–9 (2006).

Acknowledgements

We deeply acknowledge the Fédération CaSciModOT (CCSC Orléans-Tours, France), Jean-Louis Rouet and Laurent Catherine for help and access to the Région Centre computing grid. We also thanks Yann Jullian for access and help on University computer resources. This study was supported by the Région Centre-Val de Loire, France (SiSCyLi grant). Doctoral Fellow attributed to F.L. and D.D. was jointly funded by the Région Centre-Val de Loire, France and the Ministère de l'Enseignement Supérieur et de la Recherche, France.

Author Contributions

F.L., O.P., J.C., N.G. and T.D.D.B. conceived the experiment(s), F.L., D.D., O.P., M.C., S.B., V.C. and R.D.D.B. conducted the experiment(s), F.L., S.B., G.G., J.C., J.O.C. and T.D.D.B. analyzed the results. All authors reviewed the manuscript.

Additional Information

Supplementary information accompanies this paper at <https://doi.org/10.1038/s41598-018-29077-3>.

Competing Interests: The authors declare no competing interests.

Publisher's note: Springer Nature remains neutral with regard to jurisdictional claims in published maps and institutional affiliations.



Open Access This article is licensed under a Creative Commons Attribution 4.0 International License, which permits use, sharing, adaptation, distribution and reproduction in any medium or format, as long as you give appropriate credit to the original author(s) and the source, provide a link to the Creative Commons license, and indicate if changes were made. The images or other third party material in this article are included in the article's Creative Commons license, unless indicated otherwise in a credit line to the material. If material is not included in the article's Creative Commons license and your intended use is not permitted by statutory regulation or exceeds the permitted use, you will need to obtain permission directly from the copyright holder. To view a copy of this license, visit <http://creativecommons.org/licenses/by/4.0/>.

© The Author(s) 2018